Earth and Planetary Science Letters, 87 (1988) 161-172
Elsevier Science Publishers B.V., Amsterdam - Printed in The Netherlands

[5J

The combined analysis of remagnetization circles and direct observations in palaeomagnetism

P.L. McFadden and M.W. McElhinny .

Division of Geophysics, Bureau of Mineral Resources, G.P.O. Box 378, Canberra, A.C.T. 2601 (Australia)

Received January 20,1987; revised version received October 9,1987

When demagnetizing rocks in palaeomagnetism, an unterminated great circle path is sometimes obtained instead of a direct observation or endpoint determined from the linear segment near the origin of a Zijderveld plot. Such a situation cannot successfully be analysed using packages such as LINEFIND or Linearity Spectrum Analysis (LSA). It is possible to make optimum use of the great circle information by specifying constraints in the form of an arc of the great circle along which the estimate of the actual direction must lie. This specification overcomes the bias problems inherent in most analyses of converging great circles. Given M endpoints or direct observations and N great circles the maximum likelihood analysis based on all available information is easily performed. An iterative procedure is used to determine the positions of N variable-direction unit vectors so that the length, R, of the vector resultant of all $(M + N)$ unit vectors is a maximum. Standard Fisher statistics then apply, with a slight modification for the numbers of degrees of freedom. If **K** *is* the precision parameter then an approximately unbiased estimate for (1/**K**) is given by (1/k) where:

$$k = \frac{2M + N - 2}{2(M + N - R)}.$$

If α is the angle between the estimated direction and the true direction then a cone of confidence $(1 - p)$ about the mean direction has a semi-angle α_p given by:

$$\cos \alpha_p = 1 - \frac{N' - 1}{kR}\left[\left(\frac{1}{p}\right)^{1/(N'-1)} - 1\right]$$

with $N' = M + N/2$.

1. Introduction

It was recognised very early on in palaeomagnetism that rocks could contain more than one direction of magnetization and that during pjeferential demagnetization of one component the resultant direction of magnetization would move along a great circle [1,2]. In many instances individual components can be identified as linear structures in the demagnetization vector [3-5] and typically a stable endpoint (represented by a linear segment near the origin of a Zijderveld plot) is obtained. However, in some cases either because of overlap in the stability spectra of the two components and/or because the intensity decreases below the sensitivity of the measuring device, stable endpoints are not obtained and the only available information regarding the final (or "hidden") component resides in the great circle. A single great circle on its own provides insufficient information to estimate the direction of the hidden component, but if more than one great circle is available (say from different specimens) and these great circles converge, then an estimate may be obtained. Furthermore, if a direct estimate is independently available through a stable endpoint obtained from another specimen, then this may also be used to access the information available in

0012-821X/88/$03.50

a great circle. In the general case there would of course be several great circles and '(hopefully) several direct observations available.

Recognising the above, Jones et al. [6] used an analysis that combined the information from the great circles and any available direct observations, thereby providing maximum access to the information in the great circles. Subsequently Halls [7] suggested an analysis that used some of the information from the great circles, but that did not allow for a combination of the great circle information with direct observations (see also [8] and [9]). Bailey and Halls [10] then presented a separate analysis for combining great circles and direct observations. In this they incorrectly suggested that the earlier analysis [6,8] was not based on an underlying probability distribution.

Schmidt [11] presented an analysis of problems associated with bias in converging great circle methods. This problem had, to a large extent, been overcome in the early analysis [6,8] but can be a troublesome problem in the Bailey and Halls [10] analysis, particularly when there are no direct observations available. Although Schmidt noted that this bias was related to the geometrical fact that the intersections of two great circles must be 180° apart, he did not in fact identify the underlying cause of this bias within the statistical analysis. It is shown here that the bias is caused by the use of an incorrect probability distribution for the great circles,' and that we are not in a position to be able to determine the correct distribution. The approach used by Halls [7] and Bailey and Halls [10] forces them to use this incorrect distribution throughout, their analysis, causing problems with bias and their error estimation. In contrast, the earlier [6,8] analysis is flexible and allows the inclusion of further information gained in the determination of the great circle path. This information is used as a constraint that, in effect, modifies the probability distribution for each individual great circle to provide a better approximation to the true distribution for that particular great circle.

The mathematical details of the earlier [6,8] analysis were not published because it was not felt to be necessary. However, its reliability is needed in the companion paper [12] and this calls for an explanation as to why the Bailey and Halls [10] analysis is not used. Furthermore, there are several interesting points in the analysis of great circles that have not been properly discussed in the literature and presentation of the details of the earlier analysis provides a useful forum for this. The method is conceptually simple, more reliable than that presented in [10], and very easy to apply.

2. The least-squares great circle

A great circle on the (unit) sphere is of course just the intersection of the sphere with a plane through the origin. If a set of observations lie along a great circle then each of the observations lies on a plane (referred to as the great circle plane from now on)

$$px + qy + rz = 0 \tag{1}$$

where, using a superscript T to denote the transpose:

$$\boldsymbol{V} = [\,p,\, q,\, r\,]^{\mathrm{T}} \tag{2}$$

is a vector normal to this plane. $\boldsymbol{V}$ is known as the pole of the great circle and is usually specified as being a unit normal so that we have the constraint:

$$C(p, q, r) = p^2 + q^2 + r^2 = 1. \tag{3}$$

Given the n vector observations:

$$\boldsymbol{U}_i = [\,x_i,\, y_i,\, z_i\,]^{\mathrm{T}} \tag{4}$$

that define the great circle, the natural scatter will ensure that we have to determine the least-squares estimate:

$$\hat{\boldsymbol{V}} = [\,\hat{p},\, \hat{q},\, \hat{r}\,]^{\mathrm{T}} \tag{5}$$

for $\boldsymbol{V}$.

The perpendicular distance d_i from the observation $\boldsymbol{U}_i$ to the great circle plane is simply given by:

$$d_i = \boldsymbol{U}_i^{\mathrm{T}} \cdot \boldsymbol{V} = px_i + qy_i + rz_i \tag{6}$$

so that we wish to minimise the quantity:

$$D = \sum_{i=1}^{n} d_i^2. \tag{7}$$

However, this minimisation must be subject to the constraint that $p^2 + q^2 + r^2 = 1$ (otherwise the only solution would be the trivial solution $p = q = r = 0$). In other words we require the solution to the set of equations:

$$\mathrm{d}D - \lambda\, \mathrm{d}C = 0 \tag{8}$$

(C being the constraint of equation (3)). Defining the matrix **A** as:

$$\mathbf{A} = \begin{bmatrix} \sum_{i=1}^{n} x_i^2 & \sum_{i=1}^{n} x_i y_i & \sum_{i=1}^{n} x_i z_i \\ \sum_{i=1}^{n} x_i y_i & \sum_{i=1}^{n} y_i^2 & \sum_{i=1}^{n} y_i z_i \\ \sum_{i=1}^{n} x_i z_i & \sum_{i=1}^{n} y_i z_i & \sum_{i=1}^{n} z_i^2 \end{bmatrix} \quad (9)$$

equation (8) gives us the eigenvalue problem:

$$(\mathbf{A} - \lambda \mathbf{I})V = 0 \quad (10)$$

where **I** is the (3×3) unit matrix. **A** has three eigenvalues $\lambda_1 < \lambda_2 \leqslant \lambda_3$, which are the solutions to the cubic equation:

$$\det(\mathbf{A} - \lambda \mathbf{I}) = 0. \quad (11)$$

The least-squares estimate $\hat{V}$ is the eigenvector associated with the smallest eigenvalue, λ_1. This eigenvalue is easily determined using a Newton-Raphson iteration to solve (11).

2.1. Different least-squares fits and choice of weighting

Kent et al. [4] have presented an analysis for determining the linear and planar structure in palaeomagnetic remanence data. Not surprisingly their determination of any planar structure involves the least-squares estimation of a plane. However, that must not be confused with the least-squares estimation performed here. The difference is that they fit the general least-squares plane:

$$px + qy + rz = b,$$

where b is the distance from the plane to the origin, and so determine the least-squares estimate for p, q, r, and b. In general this will determine the least-squares *small* circle for the data, and this can be substantially different from the least-squares great circle. In the present application it is vital that b is constrained to be equal to zero.

Given the n observations defining a particular great circle it is natural to ask what weights should be applied to each observation in the least-squares fit. Assuming that each of the observations is known as a declination (dec_i) and inclination (inc_i), the x_i, y_i and z_i of equations (9) are given by:

$$x_i = w_i \cos(inc_i) \cos(dec_i)$$

$$y_i = w_i \cos(inc_i) \sin(dec_i)$$

$$z_i = w_i \sin(inc_i)$$

where w_i is the weight for that particular observation. It is probably quite tempting to set the w_i equal to the moment of the individual observations. However, if the two components are $\boldsymbol{M}_1$ and $\boldsymbol{M}_2$, the remanence moves from the direction of $\boldsymbol{M}_1$ to that of $\boldsymbol{M}_2$ as demagnetization proceeds, and it is not possible to obtain an endpoint, then typically $|\boldsymbol{M}_1| \gg |\boldsymbol{M}_2|$. If now the w_i are set equal to the observed moments, emphasis is placed on $\boldsymbol{M}_1$. It must be remembered that the overall object of the exercise is not, in fact, to obtain the nicest great circle, but to obtain the best estimate of the direction of $\boldsymbol{M}_2$. Consequently, if anything, the w_i should be chosen to emphasise $\boldsymbol{M}_2$ and not $\boldsymbol{M}_1$. Unfortunately the very fact that it has not been possible to isolate an endpoint indicates that the observational errors will tend to rise quite sharply as the direction of $\boldsymbol{M}_2$ is approached. Overall, therefore, the most satisfactory strategy is to set the w_i equal to unity, and duplicate that which is seen on a stereoplot.

3. The probability distributions

Consistent with most palaeomagnetic analyses the Fisher distribution [13] is assumed for the underlying probability distribution. Thus if θ is the angle between the true mean direction and a random observation then:

$$F(\theta)\, \mathrm{d}A = \frac{\kappa}{4\pi \sinh(\kappa)} \exp(\kappa \cos \theta)\, \mathrm{d}A \quad (12)$$

where $F(\theta)$ is the probability density of θ, $\mathrm{d}A$ is the differential area on the surface of the unit sphere and κ is the precision parameter.

It is assumed that the direct observations are distributed according to (12). Furthermore it is consistent to assume that in each instance where we have a great circle path but no endpoint, the endpoints would also have been distributed according to (12) had it been possible to obtain them.

Let the true mean direction be represented by the unit vector T and let ϕ be the angle between T and the pole V to a particular great circle, i.e.:

$$\cos\phi = V^{\mathrm{T}} \cdot T. \tag{13}$$

If β is the angle between the great circle and T, then $\beta = 90° - \phi$ (see Fig. 1) and we wish to determine the probability density of β. Consider now the distribution of (12), but with κ sufficiently large that we may make the approximations:

$$2\sinh(\kappa) \simeq e^{\kappa}; \quad \cos\theta \simeq 1 - (\theta^2/2)$$

giving:

$$F(\theta)\,dA \simeq \frac{\kappa}{2\pi}\exp[-\kappa(1-\cos\theta)]\,dA \tag{14}$$

from the first approximation, and together with the second:

$$F(\theta)\,dA \simeq \frac{\kappa}{2\pi}\exp(-\kappa\theta^2/2)\,dA. \tag{15}$$

As already noted, β is measured in the plane containing V, T and the origin. If α is measured along an axis perpendicular to β then, because the angles are small:

$$\theta^2 \simeq \alpha^2 + \beta^2.$$

Substituting this into (15) gives:

$$F(\alpha, \beta)\,d\alpha\,d\beta \simeq \frac{\kappa}{2\pi}\exp[-\kappa(\alpha^2+\beta^2)/2]\,d\alpha\,d\beta$$

and integrating out α to get $f(\beta)$, the probability density of β:

$$f(\beta)\,d\beta \simeq \sqrt{\frac{\kappa}{2\pi}}\exp(-\kappa\beta^2/2)\,d\beta. \tag{16}$$

Using the approximation $\cos\beta \simeq 1 - (\beta^2/2)$ gives $f(\beta)$ in the more useful form:

$$f(\beta)\,d\beta \simeq \sqrt{\frac{\kappa}{2\pi}}\exp[-\kappa(1-\cos\beta)]\,d\beta. \tag{17}$$

It is easily seen that this distribution is equivalent to that used by Bailey and Halls [10]. Taking equation (16), substituting $\cos^2\phi = \sin^2\beta \simeq \beta^2$ (since β is small) and multiplying by $\exp(\kappa)/2\sinh(\kappa) \simeq 1$ gives:

$$P(\phi)\,d\phi \simeq \frac{\exp(\kappa)\kappa^{1/2}\exp[-(\kappa\cos^2\phi)/2]}{2\cdot(2\pi)^{1/2}\sinh(\kappa)}\,d\phi,$$

which is their equation (2).

4. Maximum likelihood solution

Assuming that we have M direct observations and N great circles, and assuming that each of these is independent, the likelihood, *lik*, is given by:

$$lik = F(\theta_1)F(\theta_2)\ldots F(\theta_M)f(\beta_1)f(\beta_2)\ldots f(\beta_N).$$

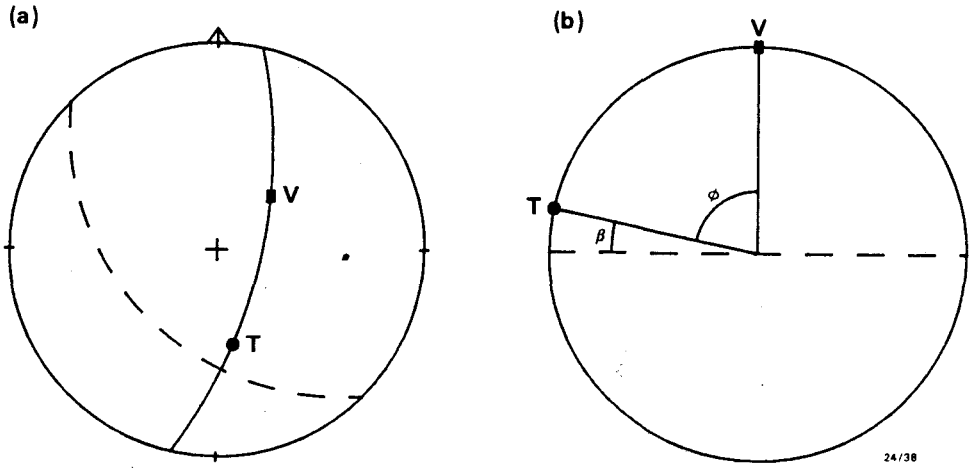

Fig. 1. Definition of angles β and ϕ. (a) Stereographic projection showing the true mean direction T and the demagnetization circle (dashed) with its pole V. The great circle joining T and V is shown solid. (b) Stereographic projection with the great circle through T and V as the primitive. The demagnetization circle (dashed) is now the equator, and the angles β and ϕ are indicated.

Using equations (14) and (17) for these distributions gives:

$$lik = \frac{\kappa^M}{(2\pi)^M} \exp\left[-\kappa \sum_{i=1}^{M} (1 - \cos\theta_i)\right] \times \frac{\kappa^{N/2}}{(2\pi)^{N/2}} \exp\left[-\kappa \sum_{j=1}^{N} (1 - \cos\beta_j)\right].$$

Letting $L = \ln(lik)$ so that L is the log-likelihood, we have:

$$L = \left(M + \frac{N}{2}\right) \ln\kappa - (M+N)\kappa + \kappa \sum_{i=1}^{M} \cos\theta_i + \kappa \sum_{j=1}^{N} \cos\beta_j - \text{const.} \quad (18)$$

Clearly the term $\Sigma \cos\theta_i = R_d$ is the sum of the projections of the unit vectors from the direct observations onto the mean direction. Similarly, $\Sigma \cos\beta_j = R_c$ is the sum of the projections of a unit vector from each great circle onto the mean direction: from the definition of the β_j it is clear that in each case the unit vector being projected is that vector on the great circle which is closest to the mean direction. With this understanding (18) takes the form:

$$L = \left(M + \frac{N}{2}\right) \ln\kappa - (M+N)\kappa + (R_d + R_c)\kappa - \text{const} = \left(M + \frac{N}{2}\right) \ln\kappa - (M+N)\kappa + R\kappa - \text{const} \quad (19)$$

with $R = (R_d + R_c)$. Apart from the very good approximation that $\exp(\kappa)/2\sinh(\kappa) \simeq 1$, equation (19) expresses exactly the same information as equation (7) of Bailey and Halls [10]. However, the presentation here is far more easily understood in physical terms, permits a more satisfactory solution and, as will be shown in section 5, allows an extension that overcomes several problems.

4.1. Estimating the remanence direction

Our aim is to determine the maximum likelihood estimate μ for the true mean direction T. Naturally this is achieved by choosing as μ that direction which maximises L, the log-likelihood. Although with the formulation used T does not appear explicitly in equation (19), for a given set of observations R is a function of T, while none of M, N or κ is a function of T. Consequently μ is simply that direction which maximises R. If there were no great circles we would have $N = 0$, $R = R_d$ and (19) would reduce to the well-known log-likelihood equation for standard Fisher statistics. R would then be maximised by choosing the direction of the vector mean of the M observed unit vectors. When there are great circles involved this direction is very easily determined by a simple iterative procedure.

In order to have an efficient iterative procedure one must be able to calculate directly that point $G = [x_g, y_g, z_g]^T$ on a great circle with pole $V = [p, q, r]^T$ which is closest to an hypothesised $\mu = [u, v, w]^T$. Letting $\rho = \cos\beta$ we have:

$$\rho = \mu^T \cdot G = ux_g + vy_g + wz_g.$$

Letting $\tau = \cos\phi$ we have:

$$\tau = \mu^T \cdot V = up + vq + wr$$

so that τ is known immediately. Since $\sin\beta = \cos\phi$ we also know ρ immediately from:

$$\rho = +\sqrt{1 - \tau^2}.$$

Since each of μ, V and G is a unit vector, this gives

$$x_g = (u - \tau p)/\rho$$
$$y_g = (v - \tau q)/\rho \quad (20)$$
$$z_g = (w - \tau r)/\rho.$$

First loop of the iteration. If there are any direct observations then the resultant, X, of these M unit vectors is determined and the unit vector $\hat{\mu}$ in the direction of this resultant vector is used as a guess for μ. If there are no direct observations available then a unit vector (as declination and inclination) is simply entered for $\hat{\mu}$. A poor guess for $\hat{\mu}$ does not affect the result (although an extremely poor guess might produce an answer 180° out, but this is obvious), it merely requires a few more iterations than for a good guess. Taking the first great circle and using equation (20), the unit vector G_1 on this great circle closest to $\hat{\mu}$ is determined. G_1 is then added to X to give a new X from which a new $\hat{\mu}$ is determined. This is then repeated for each of the great circles until X

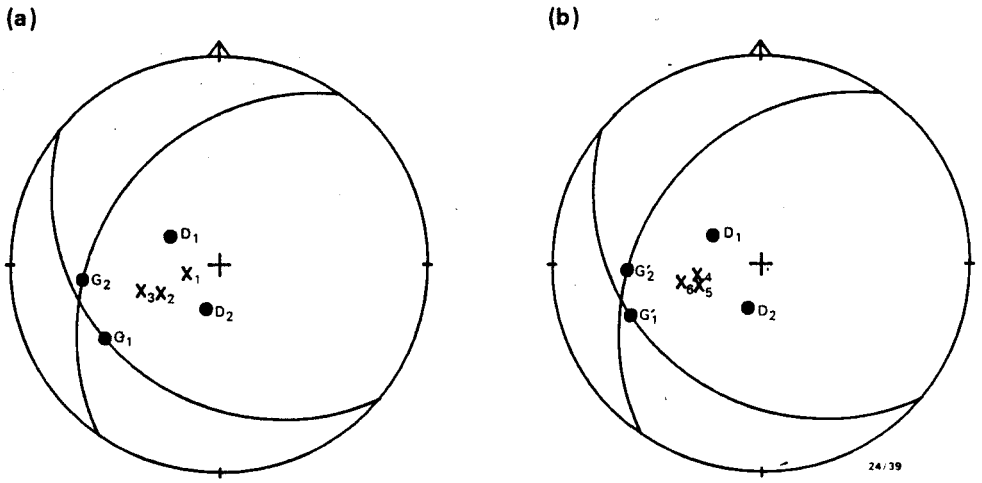

Fig. 2. Example of iteration with two set points (D_1 and D_2) and two great circles. (a) Initial loop: X_1 is the resultant of D_1 and D_2, and G_1 is the vector, on the first great circle, that is closest to X_1. X_2 is then the resultant of D_1, D_2 and G_1. G_2 is then the vector on the second great circle that is closest to X_2, leading to X_3 as the resultant of D_1, D_2, G_1 and G_2. (b) Subsequent loop: G_1 is subtracted from X_3 to give X_4 (i.e. X_4 is the resultant of D_1, D_2 and G_2). G_1' is then the vector on the first great circle that is closest to X_4, and leads to X_5 as the resultant of D_1, D_2 and G_1'. G_2' is then the vector on the second great circle that is closest to X_5, leading to X_6 as the resultant of D_1, D_2, G_1' and G_2'. G_1' and G_2' then replace G_1 and G_2 and the iteration is continued until stable positions are found for G_1 and G_2.

contains $G_1, G_2, \ldots, G_N$ (see Fig. 2a for a schematic of this process). If there were no direct observations, X will at this stage contain the unit vector entered as the original guess, and so this vector must now be subtracted from X.

Subsequent loops of the iteration. Each loop of the iteration is then as follows. G_1 is subtracted from X, a new $\hat{\mu}$ is determined from this new X, using equation (20) a new G_1 is determined (i.e. the new G_1 is the unit vector on the first great circle that is closest to the latest $\hat{\mu}$) and this is added back onto X. This process is repeated with each of the great circles so that at the end of the loop there is a new set of $G_1, G_2, \ldots, G_N$ (see Fig. 2b).

The new set of G_j values at the end of each iteration is compared with the set of G_j values at the end of the previous iteration to determine how much rotation along each great circle has occurred. Iteration continues until each of the G_j unit vectors becomes stable.

The maximum likelihood direction μ. Clearly R of equation (19) is given by:

$$R = |X| = X^T \cdot X$$

and the iteration has maximised R. Therefore μ, the maximum likelihood estimate for the mean direction is given by:

$$\mu = X/R.$$

It is important to understand that the final G_j values (i.e. those that maximised R) are the maximum likelihood estimates (on the basis of the probability distributions used) for the endpoints within the great circles (i.e. those endpoints that were not obtained during demagnetization). As shown in section 3 the probability distributions used by Bailey and Halls [10] are the same as those used here, and so these maximum likelihood estimates for the endpoints are implicit in their analysis, even though they have not derived or used them explicitly.

Naturally this gives the same estimate μ for T as the analysis of Bailey and Halls [10] but, because of the explicit use of the maximum likelihood estimates for the endpoints, is much simpler and much more easily understood.

4.2. Estimating the precision

To determine the maximum likelihood estimate $\hat{k}$ for κ, we simply differentiate L (equation (19)) with respect to κ:

$$\frac{\partial L}{\partial \kappa} = \left(M + \frac{N}{2}\right) \cdot \frac{1}{\kappa} - (M+N) + R,$$

and choose as $\hat{k}$ that value of κ which solves $(\partial L/\partial\kappa) = 0$, i.e.:

$$\hat{k} = \frac{2M+N}{2(M+N-R)}. \tag{21}$$

However, what is generally required is an unbiased estimate for κ^{-1}, and this is easily achieved by modifying equation (21). Each direct observation provides 2 degrees of freedom and each great circle provides one degree of freedom, giving a total of $(2M+N)$, the top line of equation (21). In order to estimate κ it has been necessary to obtain μ (this is needed to calculate R), thereby reducing the number of degrees of freedom by 2 to $(2M+N-2)$. Thus if we define k by:

$$k = \frac{2M+N-2}{2(M+N-R)} \tag{22}$$

then k^{-1} will be an unbiased estimate for κ^{-1}. This equation is effectively the same as equation (29) of Bailey and Halls [10] but it is easier to calculate each of the parameters here.

5. Problems with bias in estimating the mean direction

Schmidt [11] has raised the problem of bias in converging great circle methods, but the underlying cause of this bias has not been discussed. The derivation of equation (17) (section 3 and in particular see Fig. 1) shows quite clearly that there is an implicit assumption that β (or ϕ) is measured perpendicular to the great circle. Thus use of (17) for the probability density of β in determining the maximum likelihood estimate μ carries the implicit assumption that the endpoint (had it been obtainable) would have been at that point on the great circle closest to the true mean direction. Obviously in most instances the line joining the endpoint to the true mean direction is not perpendicular to the great circle and so this assumption is invalid. It is this error that leads to systematic errors in estimation (thereby causing the bias), particularly when there are no direct observations available. As has been shown, the analysis of Bailey and Halls [10] is equivalent to the analysis presented above, and their derivation confirms the presence of the invalid implicit assumption that ϕ is measured perpendicular to the great circle.

As is clear from Schmidt's [11] analysis, one needs to know the scatter about M_1, the scatter about M_2 (unknown) and the angle between M_1 and M_2 (unknown) before it is possible to determine a realistic distribution for β or ϕ (usually not measured perpendicular to the great circle). Thus it is not possible to determine the correct distribution. The Bailey and Halls [10] analysis is based only on the poles to the great circles and so cannot distinguish different points along a great circle. Thus they are unable to moderate the systematic error. In effect this means that their statistics will relate to the population of great circles, and not necessarily to the actual direction of remanence.

Because the present method makes explicit use of the maximum likelihood estimates of the unobtainable endpoints it is extremely simple to modify it to overcome most of this problem. In effect each great circle is considered simply as a constraining path for a variable unit vector during the iterative process. Thus it is a simple matter to constrain the path of the variable unit vector to a given arc of the great circle (see Fig. 3). Choice of this particular arc is subjective and is made when the least-squares fit to the great circle is performed. Given that during demagnetization the

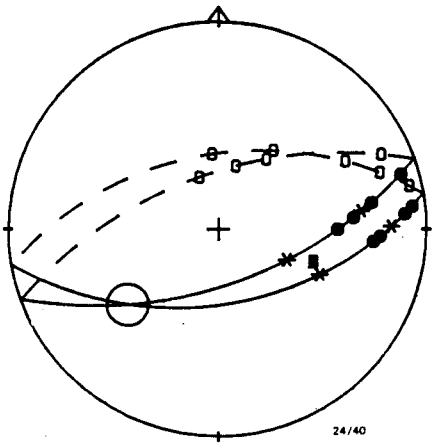

Fig. 3. Effect of sector constraints. For both great circles the motion of the resultant vector was clockwise. Without any sector constraints the solution chosen would be the intersection of the two great circles, as shown by the little circle. This result would be more than 180° along each of the great circles from their starting points. Both from this point of view and from the behaviour of the resultant vectors this result is clearly unrealistic. By defining acceptable arcs of the great circles (shown with asterisks) the result indicated by the solid square is obtained.

resultant vector moves forwards along the great circle from M_1 to M_2, it is reasonable to assume that M_2 does not lie backwards along the great circle from the last resultant vector observed. Thus, allowing for the usual scatter in observation, it is reasonable to back-up a few degrees along the great circle to a point a_1 and insist that M_2 is further forward along the great circle than this point. This point is then considered as the start of the acceptable arc for that great circle. During demagnetization it may be apparent that M_2 has almost been reached. Alternatively, comparison with other demagnetizations that resulted in end-points often allows a rough estimate to be made of how much further along the great circle the resultant vector would have drifted before stabilizing. Thus it is often possible to specify some point a_2 further forward along the great circle and be reasonable in insisting that M_2 lies between a_1 and a_2. From an operational point of view, one need not enter these points precisely. One need only enter a reasonably close guess and then using equation (20) the point on the great circle closest to this guess is used as the end of the arc. Naturally the method allows a choice to be made for each great circle as to whether an acceptable arc will be specified.

As before, the iteration is performed to maximise R, but with the additional restriction of the acceptable arcs. In practice this is achieved as follows. For the jth great circle in any iteration loop, G_j is determined exactly as outlined in section 4. If an acceptable arc has been specified it is tested whether G_j lies on the arc between a_{1j} and a_{2j}. If not, G_j is replaced by the closest of (a_{1j}, a_{2j}), and the iteration then continues as before. This then provides the maximum likelihood estimate consistent with the additional information. In effect what this does is to impose on β from each great circle its own peculiar probability distribution, which is far more realistic than the distribution of equation (17).

Initially it may be felt that there is too much subjectivity in this process and that a simple limiting to a specified arc provides too harsh a cut-off for the distribution. However, as is shown later in an example, the overall result is quite insensitive to these problems. The important aspect is that it does in fact provide a more realistic distribution for β (peculiar to each great circle) and so it does to a large extent overcome the problems of substantial bias with the use of great circles.

5.1. Consistency of great circle and direct data

Bailey and Halls [10] derived tests in an attempt to determine whether the great circles were consistent with the direct observations. To do this they obtain estimates using just the great circles and a separate set of estimates using just the direct observations. The two sets of estimates are then compared for consistency.

As shown above, when just the great circles are used with the Bailey and Halls approach, a large bias can be imposed by the analysis itself. Thus inconsistency in the estimates using their analysis does not (contrary to their claim) necessarily imply that the great circle information is inconsistent with the direct observations. As such, their consistency tests are invalid. Again this comes about because their statistics relate solely to the population of great circles, and not necessarily to the information contained therein on the remanence direction (see also [8]).

6. Confidence limits

6.1. Confidence limits for κ

Since it is not feasible to determine the real distribution for β it is similarly difficult to determine the real distribution for k. However, an approximate distribution may be determined as follows.

It is well-known that for the direct observations (e.g. see [14]):

$$2\kappa(1-\cos\theta)\cdot dist\cdot\chi_2^2$$

where "$\cdot dist\cdot$" is to be read as "is approximately distributed as". Similarly, from equation (16) or (17), it follows for the great circles that:

$$2\kappa(1-\cos\beta)\cdot dist\cdot\chi_1^2.$$

Given M direct observations, N great circles, and two degrees of freedom lost for estimating the remanence direction, this suggests that:

$$2\kappa(M+N-R)\cdot dist\cdot\chi^2_{(2M+N-2)}. \tag{23}$$

Consequently if k is defined by equation (22) then

$$\frac{\kappa}{k}(2M+N-2)\cdot dist\cdot\chi^2_{(2M+N-2)} \tag{24}$$

which was the basis for suggesting that k^{-1} is an unbiased estimate for κ^{-1}. Naturally equation (23) can be used to determine approximate confidence limits for κ.

It must be recognised that, because the proper distributions for the β are not known, the process will tend to obtain a value for R that is actually too large. This will tend to introduce bias into k so that on average it is too large. This is unfortunate but there seems little more that one can do to remedy the situation.

6.2. Confidence limits for the remanence direction

The Bailey and Halls [10] analysis produces an ellipse of confidence for the direction. Unfortunately their statistics again relate to the great circles themselves, and not to the remanence direction. A simple example shows why this is so, why they arrive at an ellipse, and why this ellipse is unreliable. Consider the example where $\boldsymbol{M}_2$ is perpendicular to $\boldsymbol{M}_1$ and where there is very little scatter in $\boldsymbol{M}_1$. Consider now a sample with several great circles and a single direct observation, which happens to be close to $\boldsymbol{M}_2$. In this situation all the poles to the great circles and the direct observation will lie very close to a single plane. Fig. 4 depicts the idealised situation where they are actually all on a single plane. Although their analysis does not explicitly use the maximum likelihood estimates for the endpoints within the great circles, these endpoints are implicit and would be where

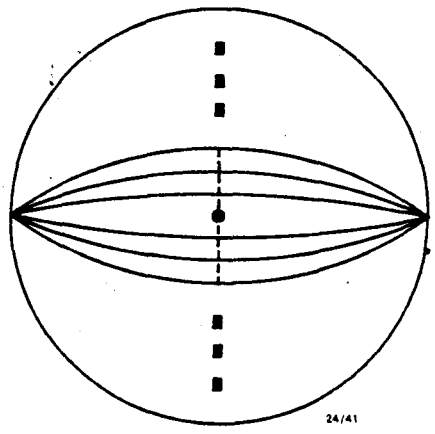

Fig. 4. If the poles (solid squares) to all the great circles and a single direct observation (solid circle) lie on a single plane, the error ellipse must collapse to a single line along the dashed line indicated.

the dotted line in Fig. 4 intersects each great circle. Thus these estimated endpoints and the direct observation would be forced by the analysis to lie very close to the single plane indicated by the dotted line. If now one considers only the scatter of the points, one obtains a very long thin ellipse (in the idealised situation of Fig. 4 this ellipse collapses to a single line along the dotted line) transverse to the great circles. This is the error ellipse determined by Bailey and Halls [10]. The important point to note is that this ascribes virtually no error along the trend of the great circles, a direction in which constraint is provided only by a single observation. A different direct observation (i.e. a different random observation from the population describing $\boldsymbol{M}_2$) would shift all of the estimated great circle endpoints and produce an error ellipse inconsistent with the first, even though the information used to determine the two error ellipses was entirely consistent.

As with κ, it is not feasible to determine a rigorous confidence limit for $\boldsymbol{T}$, the true mean direction. However, a reasonable confidence limit can be obtained by recognising that had one been able to obtain all of the endpoints by direct observation, they would have been Fisher distributed about $\boldsymbol{T}$, and the maximum likelihood estimate of the mean direction would have been Fisher distributed about $\boldsymbol{T}$ with precision (κR). Clearly a similar situation would have obtained with the maximum likelihood estimates for these great circle endpoints had we been able to use precisely correct distributions for the β. Consequently a realistic (albeit slightly inaccurate) estimate can be obtained by assuming that our maximum likelihood estimate $\boldsymbol{\mu}$ is still Fisher distributed about $\boldsymbol{T}$ with a precision of (κR). With this assumption, if α is the angle between $\boldsymbol{\mu}$ and $\boldsymbol{T}$ (i.e. $\cos\alpha = \boldsymbol{\mu}^{\mathrm{T}} \cdot \boldsymbol{T}$):

$$2\kappa R(1-\cos\alpha) \cdot dist \cdot \chi^2_2.$$

Using this distribution and the distribution of equation (23), following the analysis in [14], if α_p is the angle α will exceed with probability p, then:

$$\cos\alpha_p = 1 - \frac{N'-1}{kR}\left[\left(\frac{1}{p}\right)^{1/(N'-1)} - 1\right] \qquad (25)$$

with $N' = M + N/2$.

As an aid to fully understanding the problem of confidence limits for the mean direction consider

again the example in Fig. 4 of six parallel great circles and a single direct observation. In the direction transverse to the great circles there are seven "observations" that provide information about the location of the mean direction. Hence along this direction our estimate of the mean will be distributed about the true mean with a precision on the order of (7*k*). Without any constraints on acceptable arcs in the great circles there is only one piece of information (the direct observation) about the location of the mean in a direction parallel to the great circles. Hence along this direction our estimate of the mean will be distributed about the true mean with a precision only of about *K*. Therefore a natural confidence region for the mean would be an ellipsoid with its long axis parallel to the great circles and its short axis transverse to the circles (note the stark contrast with the Bailey and Halls ellipsoid). By having constraints on acceptable arcs in the great circles each great circle also provides information about the location of the mean in the direction parallel to the circles, thereby reducing the long axis of the natural confidence region and making it more circular. As the angle of intersection of the great circles increases, the natural confidence region will of course become more circular. Overall though, provided the estimated endpoints are realistic, the circular confidence region determined above is not unrealistic.

Because of the problems already mentioned with regard to overestimating K, there is a tendency for a_p calculated from equation (25) to underestimate the actual value. Thus it should be recognised that the actual probability of the true mean lying within the calculated confidence region will be a bit less than (1 -*p)* (i.e. typically a bit less than 95%). Unfortunately there appears to be little that one can do to improve upon this.

7. Example of analysis

The example has been chosen from the companion paper [12], and has been chosen quite specifically because it clearly illustrates the effect of including sector constraints on the great circles and the effect of including direct observations. Other examples are available in the companion paper. From the point of view of the iteration, these direct observations are nothing more than set points rather than variable points, and so they are referred to as "set points" in the example,

The example is taken from layer KB31 with 6 great circles, the results of different analyses are presented in Table 1 and illustrated in Fig. 5. In each case the motion of the resultant vector along its great circle was clockwise when viewing the figure. The result denoted *A* is from an analysis of the great circles without any sector constraints and without any set points included,

The result denoted *B* is from an analysis using sector constraints on the individual great circles, but not including any set points. A point of particular importance here is that the bounds of the sector constraints have only been run into on two of the great circles (those for KB31A4 and K.B31B1). This is quite typical and is the basis for the earlier remark that the simple limitation to a specific arc is not too harsh a cut-off for the distribution. Clearly any bounds that do appear in the solution have merely acted, in effect, as set points for the rest of the great circles,

The result denoted *C* is from an analysis not using sector constraints for the great circles but including two set points. Quite clearly the results *A* and *C* are substantially different from each other: an analysis using great circles on their own without sector constraints leads to an incorrect solution. However, the results *B* and *C* are not substantially different, and the inclusion of sector constraints in the *B* analysis has substantially reduced the problems with bias,

The result denoted *D* is from an analysis using the sector constraints on each of the great circles and also using the two set points. It is interesting to note that one of the sector constraints has come into play here (on KB31D1). However, it is the constraint at the start of the acceptable sector, whereas previously it was the constraints at the *end* of the acceptable sector. In this particular instance the set points have tried to pull the variable point too far back along the great circle —precisely the opposite of what was happening without the set points. In this particular example the resuit *D* is so close to the result *C* that they are not visually distinguishable,

It is worth noting at this stage that a linear decay to the origin of a Zijderveld diagram is not always a good indication of a true direction. As seen in the above example, with several subparal-

TABLE 1

Effect of sector constraints and direct observations

Great circle analysis for KB 31

Set point data (number of set points = 2)			Great circle information (number of great circles = 6)					
Specimen	D (°)	I (°)	Specimen	Eigenvectors			Constraints	
				p	q	r	D/I	D/I
KB31A3	146.6	−52.6	KB31A1	0.263	0.664	−0.700	180.0/−20.6	260.0/−45.0
KB31B3	195.5	−57.9	KB31A4	0.794	0.335	−0.507	141.0/−38.7	200.0/−59.5
			KB31B1	0.692	0.358	−0.627	134.7/−20.3	196.6/−50.7
			KB31C2	0.593	0.663	−0.457	148.0/−18.4	210.0/−61.6
			KB31D1	0.637	0.476	−0.606	190.0/−49.5	270.0/−38.1
			KB31D2	0.628	0.524	−0.576	157.0/−32.9	215.0/−54.7

Great circle results			Overal results	Great circle results			Overal results
Specimen	D (°)	I (°)		Specimen	D (°)	I (°)	
Analysis A: no sector constraints, no set points				*Analysis C: set points, no sector constraints*			
KB31A1	246.8	−45.6	$D = 246.8°$, $I = -50.5°$	KB31A1	200.6	−34.4	$D = 183.1°$, $I = -51.2°$
KB31A4	246.9	−50.7	$N_{total} = 6$	KB31A4	179.7	−57.3	$N_{total} = 8$
KB31B1	242.7	−45.4	$R = 5.9735$	KB31B1	184.3	−48.8	$R = 7.8336$
KB31C2	252.9	−60.5	$k = 75.592$	KB31C2	180.8	−52.8	$k = 24.032$
KB31D1	245.8	−48.9	$\alpha_{95} = 10.1°$	KB31D1	185.3	−48.2	$\alpha_{95} = 12.5°$
KB31D2	247.5	−51.5		KB31D2	184.7	−49.3	
Analysis B: sector constraints, no set points				*Analysis D: set points and sector constraints*			
KB31A1	212.4	−39.5	$D = 202.3°$, $I = -52.5°$	KB31A1	201.9	−35.1	$D = 184.8°$, $I = -51.7°$
KB31A4	200.0	−59.5 *	$N_{total} = 6$	KB31A4	181.6	−57.7	$N_{total} = 8$
KB31B1	196.6	−50.7 *	$R = 5.9491$	KB31B1	186.0	−49.2	$R = 7.8325$
KB31C2	196.8	−59.0	$k = 39.307$	KB31C2	182.3	−53.6	$k = 23.874$
KB31D1	202.5	−51.8	$\alpha_{95} = 14.0°$	KB31D1	190.0	−49.5 *	$\alpha_{95} = 12.5°$
KB31D2	201.9	−53.5		KB31D2	186.3	−49.8	

* Denotes the end of an acceptable sector.

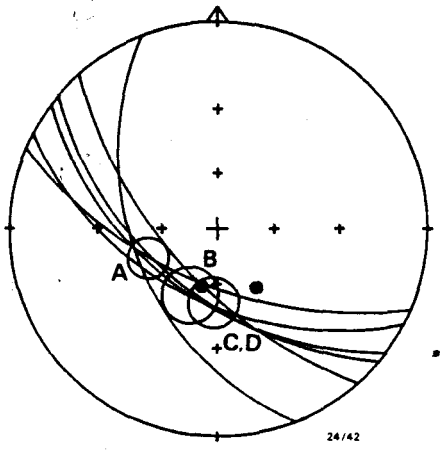

Fig. 5. Analyses of 6 great circles from layer KB31. *A*: No sector constraints used and no set points included. *B*: Sector constraints used but no set points included. *C*: No sector constraints used but set points included. *D*: Sector constraints used and set points included. Solid circles are the two set points and the open circles represent the circles of 95% confidence for the results *A*, *B*, *C* and *D*.

lel great circles the estimate for the mean direction is strongly dependent on the position of the direct observation(s), and this places a heavy responsibility upon the reliability of the direct observation(s). In all instances, a direction estimated from great circles intersecting each other at large angles must be considered as inherently more reliable than a direction estimated from sub-parallel great circles.

8. Conclusions

A method for the combined analysis of remagnetization circles and direct observations has been formulated that overcomes some fundamental problems present in the technique proposed by Bailey and Halls [10]. The statistical formulation of the problem as posed by Bailey and Halls [10] relates specifically to the population of great circles

and not to the remanence directions themselves. Thus it is very difficult to have any intuitive feeling for what is taking place during the analytical process. Their technique derives an ellipse of confidence that is based on an analysis of the poles of the great circles: this is shown to be unrealistic as it ignores available information.

The method proposed here is a physically intuitive one in which the process can easily be followed during iteration. The analysis provides maximum likelihood estimates based on *all* of the available information: the addition of realistic sector constraints to the great circles (based on the observed remanence directions) effectively overcomes the bias caused in the Bailey and Halls method [10,11]. The statistical analysis is very simple as it is based on the commonly used and well-known Fisher [13] distribution. Thus the final estimate of the mean direction has a circle of confidence associated with it. The only modification to standard Fisher statistics is in the number of degrees of freedom: this is because knowledge of the great circle provides less information (in fact, only one degree of freedom) than the information available (two degrees of freedom) with a direct observation.

Acknowledgements

The presentation of this paper has benefited from the comments of anonymous reviewers. This paper is published with the permission of the Director, Bureau of Mineral Resources, Geology and Geophysics.

References

1 K..M. Creer, A preliminary palaeomagnetic survey of certain rocks in England and Wales, 203 pp., unpublished Ph.D. Thesis, University of Cambridge, 1955.

2 A.N. Khramov, Palaeomagnetism and Stratigraphic Correlation, Gostoptechizdat, Leningrad, 1958 (English translation by A.J. Lojkine, E. Irving, ed., Geophysics Department, Australian National University, 1960).

3 J.L. Kirschvink, The least-squares line and plane and the analysis of palaeomagnetic data, Geophys. J. R. Astron. Soc. 62, 699-718, 1980.

4 J.T. Kent, J.C. Briden and K..V. Mardia, Linear and planar structure in ordered multivariate data as applied to progressive demagnetization of palaeomagnetic remanence, Geophys. J. R. Astron. Soc. 75, 593-621, 1983.

5 P.W. Schmidt, Linearity spectrum analysis of multi-component magnetizations and its application to some igneous rocks from south-eastern Australia, Geophys. J. R. Astron. Soc. 70, 647-665, 1982.

6 D.L. Jones, I.D.M. Robertson and P.L. McFadden. A palaeomagnetic study of Precambrian dyke swarms associated with the Great Dyke of Rhodesia, Trans. Geol. Soc. S. Afr. 78, 57-65, 1975.

7 H.C. Halls, A least-squares method to find a remanence direction from converging remagnetization circles, Geophys. J. R. Astron. Soc. 45, 297-304. 1976.

8 P.L. McFadden, Comments on "A least-squares method to find a remanence direction from converging remagnetization circles" by H.C. Halls, Geophys. J. R. Astron. Soc. 48. 549-550, 1977.

9 H.C. Halls, Reply to P.L. McFadden's comment. Geophys. J. R. Astron. Soc. 48, 551-552, 1977.

10 R.C. Bailey and H.C. Halls, Estimate of confidence in paleomagnetic directions derived from mixed remagnetization circle and direct observational data. J. Geophys. 54. 174-182. 1984.

11 P.W. Schmidt, Bias in converging great circle methods. Earth Planet. Sci. Lett. 72, 427-432. 1985.

12 P.L. McFadden, X.A. Ma, M.W. McElhinny and Z.K. Zhang, Permo-Triassic magnetostratigraphy in China: northern Tarim. Earth Planet. Sci. Lett. 87, 152-160. 198X (this issue).

13 R.A. Fisher, Dispersion on a sphere, Proc. R. Soc. London. Ser. A 217, 295-305, 1953.

14 P.L. McFadden, Determination of the angle in a Fisher distribution which will be exceeded with a given probability, Geophys. J. R. Astron. Soc. 60, 391-396, 1980.